



*senseable* city lab:...

## On thermally forced flows in urban street canyons

S. Magnusson · A. Dallman · D. Entekhabi ·  
R. Britter · H. J. S. Fernando · L. Norford

Received: 24 September 2013 / Accepted: 19 March 2014 / Published online: 3 April 2014  
© Springer Science+Business Media Dordrecht 2014

**Abstract** During sunny days with periods of low synoptic wind, buoyancy forces can play a critical role on the air flow, and thus on the dispersion of pollutants in the built urban environments. Earlier studies provide evidence that when a surface inside an urban street canyon is at a higher temperature than that of local ambient air, buoyancy forces can modify the mechanically-induced circulation within the canyons (i.e., gaps between buildings). The aspect ratio of the urban canyon is a critical factor in the manifestation of the buoyancy parameter. In this paper, computational fluid dynamics simulations are performed on urban street canyons with six different aspect ratios, focusing on the special case where the leeward wall is at a greater temperature than local ambient air. A non-dimensional measure of the influence of buoyancy is used to predict demarcations between the flow regimes. Simulations are performed under a range of buoyancy conditions, including beyond those of previous studies. Observations from a field experiment and a wind tunnel experiment are used to validate the results.

**Keywords** Buoyancy dominant flow · Buoyancy parameter · CFD simulations · Urban street canyons

---

S. Magnusson (✉) · D. Entekhabi  
Department of Civil- and Environmental Engineering, Parsons Laboratory,  
Massachusetts Institute of Technology, Cambridge, MA 02139, USA  
e-mail: siggipm@mit.edu; sigurdur.petur.magnusson@gmail.com

S. Magnusson · D. Entekhabi · R. Britter · L. Norford  
Center for Environmental Sensing and Modeling, Singapore-MIT Alliance for Research  
and Technology, Singapore 138062, Singapore

A. Dallman · H. J. S. Fernando  
Department of Civil- and Environmental Engineering and Earth Sciences,  
University of Notre Dame, Notre Dame, IN 46556, USA

R. Britter · L. Norford  
Department of Architecture, Building Technology Program, Massachusetts Institute of Technology,  
Cambridge, MA 02139, USA

## 1 Introduction

By the end of 2008, for the first time in human history, more than 50 % of the earth's population lived in urban areas, and this is expected to rise to 70 % by 2050 (UN DESA [8]). The urban air quality and its impact on public health have long been known, but with increasing urbanization the control and mitigation of health impacts has raised awareness on related issues. Fundamental understanding of flow and dispersion in urban canyons is a necessary element in predicting exposure levels. The complex morphology of urban building structures and connective roads requires an understanding of turbulence within the resulting urban canyons. The use of dense construction material with low albedo leads to sustained elevation of surface temperatures. Hence buoyancy effects may be as important as mechanically-forced or shear-induced flows. In a review paper by Britter and Hanna [3], pertinent research has been divided into flow on the street scale, the neighborhood scale, the city scale and the regional scale. Studies at each scale are described as: (i) the street scale (less than 200 m) mainly deals with air quality issues, where emissions from vehicles are most often the source of pollutants; (ii) the neighborhood scale is of size 1–2 km, wherein detailed computational studies of turbulence are still feasible; (iii) the city scale (20–30 km) is characterized by buildings that lead to a high drag force or reduced wind in the urban area as well as large thermal storage; and (iv) regional scale (up to 200 km) is an area where large-scale pressure gradients are prominent and synoptic flow prevails. This study focuses on the street scale, which can be considered an elemental urban canyon with buildings adjacent to a surface road.

The combination of mechanical and buoyancy effects characterizes the flow within an urban canyon. The magnitude of mechanical forcing within an urban airshed depends on the synoptic wind conditions and building configuration, while buoyancy forcing depends on the temperature differences between the urban surfaces and ambient air that drive sensible heat fluxes. Three heat exchange mechanisms exist, with different impacts on the stability of the near-surface urban air: first, a neutral condition with no sensible heat fluxes; second, an unstable condition with a heat flux from the surface to ambient air; and finally, a stable condition where there is a heat flux from air to the surface. In this study we focus on daytime conditions where solar radiation heats the buildings and road surfaces significantly. The study is therefore limited to unstable regimes but neutral conditions are included as a reference for the comparison of cases, including additional buoyancy forcing on the flow. The urban area is simplified into a two-dimensional urban street canyon, shown in Fig. 1. The temperature difference between the near-surface air and the ambient and inner canyon fluids leads to buoyancy fluxes within and across the canyon.

The paper is divided into six sections. Section 2 covers relevant literature, followed by theoretical considerations in Sect. 3. Section 4 describes the CFD simulations, and the main results are in Sect. 5. The conclusions are given in Sect. 6.

## 2 Background

There have been limited foundational studies of buoyancy effects in urban canyons. In this section we review their major findings and define the launching point for this study based on them. The traditional way to quantify the interaction between the buoyancy and the mechanical forces is to consider the Richardson number ( $Ri$ ). Within the canyon,  $Ri$  is defined in Li et al. [12] and Turner [22] as

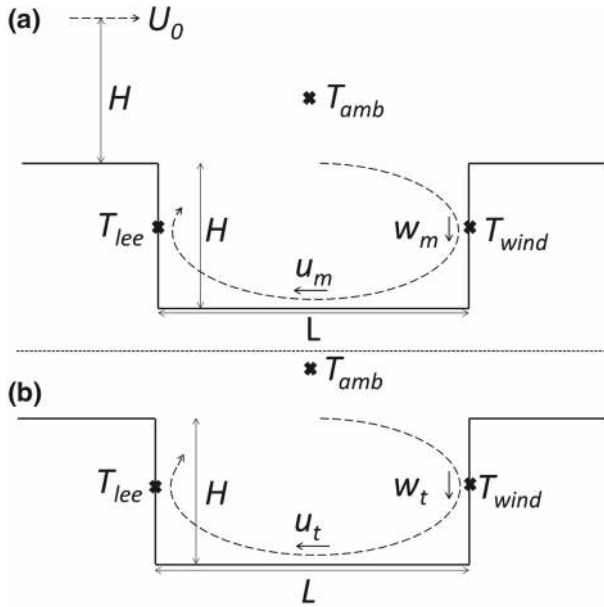


**Fig. 1** **a** Predicted flow inside the urban street canyon when the windward wall, the leeward wall and the ambient air are at an identical temperature (isothermal). **b** No free stream flow exists, and the temperature of the leeward wall is at a higher temperature than the temperature of the windward wall, which is at the same temperature as the ambient air above the canyon. If the buoyancy case is added to the isothermal case, the thermal conditions assist the mechanically driven flow where two vortices are rotating in the same direction, leading to larger air speeds inside the canyon

$$Ri = - \left( \frac{g (T_{walls} - T_{amb}) H}{T_{amb} U_0^2} \right), \tag{1}$$

where  $g$  is the gravitational acceleration ( $\text{ms}^{-2}$ ),  $T_{walls}$  the average temperature of the canyon walls (K),  $T_{amb}$  the ambient air temperature (K),  $H$  the height of the canyon (m), and  $U_0$  the free stream velocity above the canyon ( $\text{ms}^{-1}$ ).

In Fernando et al. [9] the aspect ratio of the canyon is taken into the definition of  $Ri$ . The thermal driving force inside the canyon is considered to be the average temperature difference between the walls and air ( $T_{walls} - T_{amb}$ ) and thus the buoyancy driven circulation characterized by  $\left( \frac{g(T_{walls} - T_{amb})}{T_{amb}} \right)$ . This buoyancy driven circulation competes with the mechanically forced circulation,  $u_c$ , inside the canyon which is driven by the overlying flow,  $U_0$ . From simple kinematics (mass balance) we have  $\frac{\partial u}{\partial x} \sim \frac{\partial w}{\partial z}$ , where  $u$  and  $w$  are the characteristic in-canyon horizontal and vertical velocities of the flow. Thus,  $\frac{U_0}{L} \sim \frac{w}{H}$  which leads to  $w \sim u_c \sim U_0 \frac{H}{L}$ . The balance between the buoyancy and mechanical effects is given by the canyon Richardson number in Fernando et al. [9]

$$Ri_c = - \left( \frac{g (T_{walls} - T_{amb}) H}{T_{amb}} \right) / u_c^2 = - \left( \frac{g (T_{walls} - T_{amb}) H}{T_{amb} U_0^2} \right) \left( \frac{L}{H} \right)^2, \tag{2}$$

where  $L$  is the width of the canyon (m) and  $H/L$  the aspect ratio of the canyon. Fernando et al. [9] state that according to numerical simulations performed by Sini et al. [19] the canyon flow is buoyancy dominated when  $Ri_c$  is greater than 0.5–1.0.

Sini et al. [19] developed and implemented the numerical model CHENSI to simulate air flow inside an urban street canyon as well as vertical exchange of pollutants between the canyon and ambient air. The model showed that the differential heating of the walls influences the air exchange at the roof level (top interface) and, consequently, air quality and human exposure to pollutants within the street canyon. In addition, the model predicted various flow structures, depending on the wall temperatures. In this early study the absolute value of  $Ri$  was low ( $< 10.0$ ) compared to values explored in this study. Later, Kim and Baik [10] investigated the thermal effects on air flow and pollutant dispersion in street canyons for various aspect ratios. The simulations were performed for lower  $Ri$  than considered in our study. The effects of temperature differences between the street and the ambient air, the windward wall and the ambient air, and the leeward wall and ambient air were investigated. When the leeward wall was heated, only one vortex formed inside the canyon, regardless of the aspect ratio and thermal conditions. When the windward wall was heated, two vortices could be formed, depending on the aspect ratio. Li et al. [12, 13] performed large-eddy simulations of flow in an urban street canyon, with heating of the street surface. They found that street heating significantly enhanced the mean flux, turbulence and turbulent fluxes inside the canyon. The modulus of  $Ri$  for their simulations was limited to 2.4.

The effects of the buoyancy flux due to heated walls in an urban street canyon were investigated in a real urban street canyon in Nantes, France, by Louka et al. [14, 15]. They found that the effects of wall heating were only important for the near wall flow. CFD simulations were also performed by Louka et al. [15], but these simulations overestimated the effects of the heating of the windward wall. In complementary wind tunnel measurements of Allegrini et al. [1], an urban street canyon with a differential wall heating was considered for three different Reynolds numbers ( $Re$ ). For the windward heated case when  $Re$  is 9,000, two main counter-rotating vortices were formed, in agreement with CFD simulations of Louka et al. [15]. The wind tunnel measurements show how the leeward wall heating leads to accelerated rotation of a single vortex.

Solazzo and Britter [20] performed CFD simulations on a two-dimensional urban street canyon with heating of all three canyon surfaces, for  $-0.1 < Ri < 0$ . In-canyon air temperature was uniformly distributed except near the heated wall, and thus the contribution of the heated wall to the flow as a whole was minimal. On the other hand, Fernando et al. [9] presented three-dimensional CFD simulations on the thermal effects of a downtown area in Phoenix. The results showed significant buoyancy effects all the way to the middle of the canyon at tens of meters above the ground. The mismatch can be partially explained by the greater height of the buildings in the downtown area that leads to higher calculated  $Ri$ . Also, in a complex geometry as in the downtown area of Phoenix, low wind ‘dead zones’ in the wakes behind the taller buildings are more affected by buoyancy fluxes.

Cai [4, 5] performed large eddy simulations (LES) under differential wall heating conditions, where  $|Ri|$  was limited to 2.14. The vortex rotation was accelerated when the leeward wall was heated and was suppressed by the heating of the windward wall.

Similar LES studies of Park et al. [17] showed that heating of the leeward wall and the street leads to increased air speeds in the canyon, while heating of the windward wall leads to a smaller mechanically driven vortex and an extra thermally driven vortex near the windward wall, rotating in a different direction compared to the mechanically driven vortex. The  $Ri$  was small compared to simulations presented in our study.

In the current study we show how the in-canyon flows are affected by leeward wall heating. The CFD simulations are performed for urban street canyons of six aspect ratios, and these cover all flow categories of Oke [16]: isolated roughness flow, wake interference flow and skimming flow.

For further validation, one of the street canyons simulated has the same aspect ratio (0.67) as the canyon considered in the field experiment of Dallman et al. [7]. For this aspect ratio the flow is in transition from wake interference to the skimming flow regimes. We include the observed ranges of heating and buoyancy, but extend the simulations to explore a wider range of conditions than observed in the short-duration field experiment. The special case of  $U_0 = 0$  was also investigated.

We aim to classify the flow into mechanically and buoyancy driven flows, with an intermediate (transition) regime in between. We also explore conditions where buoyancy effects are larger than in previous studies. The flow regimes and transitions between them are shown to be captured by a nondimensional number that includes the degree of mechanical forcing, thermal contrasts and canyon geometry. Finally we estimate the buoyancy effects on turbulent eddy viscosity ( $\nu$ ) inside the canyon, which is useful for gaining basic insights into the effects of buoyancy on pollutants and human exposure to particulates in urban canyon settings.

### 3 Theoretical considerations

Dallman et al. [7], introduced results from a field experiment in Singapore that was conducted during the summer of 2012. The flow inside an artificial urban street canyon, made of two rows of aligned shipping containers, was measured and the thermal effects estimated. Wind velocities, eddy heat fluxes and wall temperatures were measured in the constructed canyon and in the ambient air above it. Furthermore, a smoke machine was used to visualize the flow. A non-dimensional buoyancy parameter,  $B$  was introduced to evaluate the buoyancy effects on the flow:

$$B = \left( \frac{g \Delta T_{walls} H}{T_{amb} U_0^2 [1 + (H/L)^2]} \right) \tag{3}$$

where  $\Delta T_{walls} = T_{lee} - T_{wind}$  is the temperature difference between the canyon walls (K),  $H$  the height of the canyon (m),  $T_{amb}$  the ambient air temperature (K), and  $U_0$  the free stream velocity above the canyon ( $\text{ms}^{-1}$ , defined at  $1 H$  above the canyon to be consistent to Dallman et al. [7]). This parameter is comparable with  $Ri$ , used for example in Li et al. [12]. The difference is that  $Ri$  accounts for temperature differences between a surface of the street canyon and the ambient air, while the  $B$  parameter accounts for temperature differences between side walls of the canyon. The temperature difference between the walls is believed to impact the formation of a vortex inside the urban street canyon. The aspect ratio ( $H/L$ ) modulates the buoyancy parameter and hence the flow regime conditions. The  $B$  parameter does not distinguish which wall inside the canyon is at a larger temperature. When the leeward wall is heated, buoyancy-driven flow occurs in the same direction as the mechanically-induced flow inside the canyon (assisting flow), but when the windward wall is heated the buoyancy flow is in the opposite direction to the mechanically-induced flow. In this study, the focus is on the case when only the leeward wall is heated.

The goal of our simulations is to evaluate the effects of different wall heating conditions. To this end, the flow is classified into two limiting regimes: mechanically and buoyancy driven. A critical buoyancy parameter ( $B_c$ ) was defined (Dallman et al. [7]) where the transition from one regime to another occurs through an intermediate regime. In the case where the leeward wall is heated, Dallman et al. [7] deduced the relationship between  $B$  and the characteristic in-canyon horizontal velocity,  $u$ , for buoyancy driven flow in the skimming regime (Oke [16]). Dallman et al. [7] use vorticity generation to show that the buoyancy driven velocity

inside the canyon is a function of the buoyancy parameter raised to the power of 0.5. The mechanically driven flow inside the canyon is linearly proportional to the free stream flow above the canyon. Thus, the characteristic in-canyon horizontal velocity of the vortex inside the canyon scales with  $B$  as:

$$\frac{u}{U_0} \sim \begin{cases} u_m/U_0 \approx \gamma_1 & B < B_c \\ u_t/U_0 \approx \gamma_2 B^{1/2} & B > B_t \end{cases} \quad (4)$$

where  $u$  is the characteristic in-canyon horizontal velocity inside the canyon,  $U_0$  the free stream flow velocity above the canyon as before,  $u_m$  the characteristic in-canyon mechanically driven horizontal velocity inside the canyon (Fig. 1),  $u_t$  the characteristic horizontal buoyancy driven in-canyon velocity inside the canyon (Fig. 1),  $\gamma_1$  and  $\gamma_2$  are constants,  $B_c$  the critical buoyancy parameter and  $B_t$  a critical value of  $B$  where the flow is completely buoyancy (thermally) dominated. Between the two limiting regimes, an intermediate regime is expected ( $B_c < B < B_t$ ), where the flow depends on the free stream velocity and differential heating. Simple linear superposition gives a parameterization for the velocity in the intermediate regime,

$$\frac{u}{u_0} \approx \gamma_3 + \gamma_4 B^{1/2}. \quad (5)$$

In Dallman et al. [7], the characteristic in-canyon horizontal velocity,  $u$ , is measured by a weather station at the lower part of the canyon. One of our goals is to estimate the critical  $B$  parameter and to examine if the buoyancy driven flow is a function of  $B^{1/2}$  as theoretically predicted. CFD simulations are applied to investigate these considerations.

#### 4 The CFD simulations

The computational domain is shown in Fig. 2. The free stream velocity above the canyon is characterized by a horizontal velocity  $U_0$  that is defined to be perpendicular to the urban street canyon (normal to its axis) and is defined at  $1 H$  above the roof of the canyon to be consistent with the measurements in Dallman et al. [7]. The buoyancy flow is driven by the difference in temperature between the two walls and ambient air. The temperatures of the walls are  $T_{lee}$  and  $T_{wind}$ , and the ambient air above the canyon temperature is  $T_{amb}$ . The street temperature is denoted by  $T_{street}$ .

The finite volume CFD code ANSYS FLUENT 13.0 is used in this study. The standard  $k - \varepsilon$  turbulence closure is used to solve the Reynolds-averaged Navier–Stokes equations of the fluid flow. The transport equations for the turbulence kinetic energy,  $k$ , and the rate of dissipation,  $\varepsilon$ , can be found in the Ansys Theory Guide [2]. Full buoyancy effects are used in the standard  $k - \varepsilon$  turbulence model, so buoyancy effects are included in  $k$  and the dissipation rate,  $\varepsilon$ , equations. The density of air is calculated using the Boussinesq approximation. The CFD model is integrated until steady-state conditions are achieved. The air flow is considered to be steady when the fluid parcel has made several complete circuits inside the canyon, i.e., the time scale is larger than  $H/u$ . In the field experiment, the problem is dynamic and more complex. The field experimental data (Dallman et al. [7]) used for comparison are considered to be steady or near steady when the flow is normal to the canyon axis ( $\pm 15^\circ$ ) for at least 30 seconds (approximately three circulations of a fluid parcel). The temperature difference between the walls is considered to be constant during this period and thus the flow is quasi-steady. The CFD simulations were considered converged when the scaled simulated residuals were less than  $10^{-6}$ .

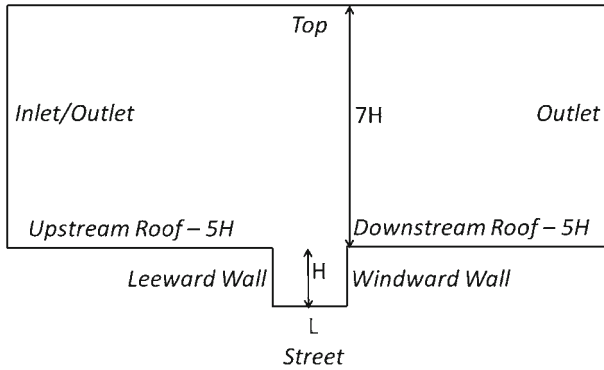


**Fig. 2** The computational domain for the urban street canyon is defined as a cavity in a flat plate, thus excluding flow separation at the edge of the upstream building

The canyon is simulated as a smooth wall cavity with height  $H$  and width  $L$  ( $H$  is 2.5 m and  $L$  varies between the simulations in order to produce different canyon aspect ratios). We perform CFD simulations that extend beyond the experimental setting of Dallman et al. [7]. The purpose is to investigate the physical effects of the different wall heating configurations on the air flow inside the canyon. Specifically we investigate the development of varying flow regimes for different values of the  $B$  parameter. In the field experiment in Dallman et al. [7], two obstacles (containers) rise above the ground which leads to separation of the flow at the edge of the upstream obstacle. Because of the complex landscape around the experimental site (trees, buildings, an industrial site and fences) and lack of information on the oncoming velocity profile, the cavity approach is considered to be better suited for the purpose of this study. We aim to isolate the effect of the  $B$  parameter from flow separation above the canyon. The experimental results indicate that the flow is reattached at the roof of the upstream building which makes the cavity approach relevant. Also the laboratory experiment performed by Allegrini et al. [1] is closer to the setting of the CFD simulations (cavity approach).

The height of the computational domain above the canyon is  $7H$ , and its upstream and downstream extents are  $5H$ . Ansys Inc. recommends that the height, the upstream length and the downstream length of a computational domain are not less than five times the height or the diameter of the obstacle.

The mechanical boundary conditions are the following at the inlet: the wind velocity, turbulent kinetic energy and turbulent dissipation rate profiles are defined as in Richards and Hoxey [18]

$$U(z) = \frac{u_*}{\kappa} \ln \left( \frac{z + z_0}{z_0} \right), \tag{6}$$

$$k(z) = \frac{u_*^2}{\sqrt{C_\mu}}, \tag{7}$$

$$\varepsilon(z) = \frac{u_*^3}{\kappa(z + z_0)}, \tag{8}$$

where  $z$  is the height above the roof (m),  $u_*$  the friction velocity ( $\text{ms}^{-1}$ ),  $\kappa$  the von Karman constant (0.40),  $z_0$  is the roughness length of the urban terrain, meant to reflect to the effects of the roughness of the surface (in this case the buildings) on the wind flow. For an area of



few buildings and many trees as at the experimental site in Dallman et al. [7]  $z_0$  is set as 0.25 m, following Stull [21].  $C_\mu$  is a constant in the standard  $k - \epsilon$  model. The outlet has a zero gauge pressure which means that the pressure difference across the boundary is zero and the air flow thus horizontal at this vertical boundary. The top boundary is defined as a wall with no shear stress. The upstream and downstream roofs, the street and the two walls are defined as smooth walls with no-slip shear conditions. In the special case when  $U_0$  is set to zero, the inlet is defined as a pressure outlet with a zero gauge pressure as well.

The thermal boundary conditions are the following: the temperatures of inflow air at the inlet boundary and backflow air at the outlet are set as  $T_{amb}$  (300 K). The temperatures of the street ( $T_{street}$ ), windward wall ( $T_{wind}$ ), upstream ( $T_{uproof}$ ) and downstream ( $T_{downroof}$ ) roofs and the top ( $T_{top}$ ) boundaries are all set to the same temperature as the ambient air. The temperature of the leeward wall ( $T_{lee}$ ) is kept constant and the gravity vector is changed using successive steady state steps.  $Re$  of the flow is about 40,000, so the flow is  $Re$  independent; according to Castro and Robins [6], a flow around a surface-mounted cube becomes  $Re$  independent for  $Re > 30,000$ .

The Ansys Fluent Workbench mesh generator is used to configure the CFD model. The cells are quadrilateral and smaller grid sizes are defined near the surfaces of the computational domain. Larger grid sizes are permitted at distances away from the surfaces [2]. The mesh resolution for the computational domain expands from 0.025 to 0.1  $H$  with an expansion factor of 1.05. The standard wall function is applied which is the default setting in Fluent. Sensitivity experiments were performed to ensure that the computational domain and the mesh resolution do not bias the results.

Figure 1 is an illustration of the flow inside the urban street canyon under two conditions. The upper panel shows a vortex formed under mechanical forcing. The lower panel illustrates a buoyancy driven case, with no background winds. The temperature difference between the two walls leads to the formation of a vortex inside the canyon. If the temperature difference from the lower panel is added to the mechanical case, it is believed that the buoyancy driven flow assists the formation of a vortex.

## 5 Results

A goal of the CFD simulations is to investigate the relationship between a characteristic velocity ( $u$ ) inside a canyon and the  $B$  parameter introduced in Dallman et al. [7] and shown in Eqs. (4) and (5). Thus we introduce the following equations to compare the constants from each method:

$$\frac{u}{U_0} = \begin{cases} a_1 & B \leq B_c \\ a_2 + a_3 B^{b_1} & B_c \leq B \leq B_t \\ a_4 B^{b_2} & B \geq B_t \end{cases} \quad (9)$$

where  $a_1$ ,  $a_2$ ,  $a_3$ ,  $a_4$ ,  $b_1$  and  $b_2$  are constants that will be determined from the CFD simulations,  $B_c$  is the critical buoyancy parameter  $B$  for buoyancy effects to set in and  $B_t$  is the critical  $B$  for the flow to become completely buoyancy dominated. The in-canyon velocity,  $u$ , is measured as the average horizontal velocity inside a box from 0.1  $H$  above the street up to 0.4  $H$  above the street canyon, and 0.35  $L$  from the leeward wall up to 0.65  $L$ , as shown in Fig. 3. The velocity at this position in the canyon is considered to be characteristic of the strength of the vortex (bulk flow) and to be consistent with  $u$  in Allegerini et al. [1], Dallman et al. [7] and Park et al. [17] which was measured in the lower part of the canyon.

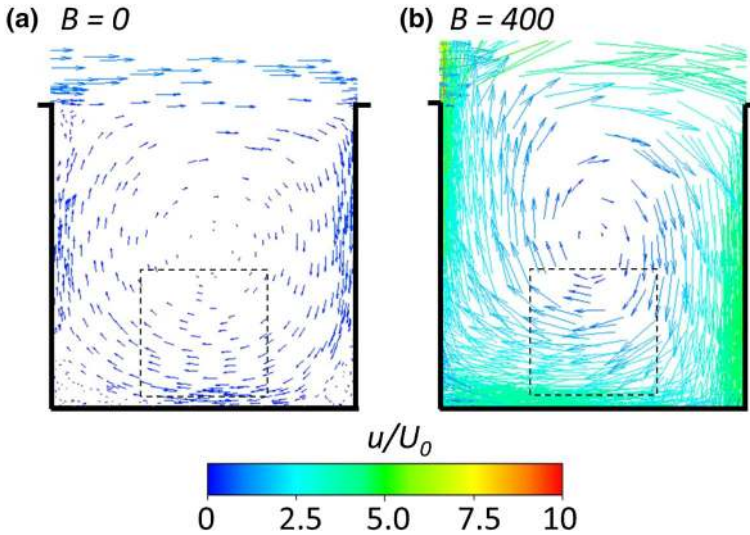


**Fig. 3** The vector field for two values of the  $B$  parameter, with the leeward wall heated in a canyon with aspect ratio 1. The region of the strong upward velocity at the heated leeward side is very thin, approximately  $0.01 H$ . The boxes show where  $u$  is measured, from  $0.1$  up to  $0.4 H$  (vertically) and between  $0.35$  and  $0.65 L$  (horizontally)

Simulations with  $U_0 \neq 0$  and a heated leeward wall have a combination of mechanical and buoyancy flows. The CFD simulations are performed for the buoyancy parameter between 0 and 400. This extends the physically realizable range and thus includes extreme cases. Figure 3 shows the velocity vectors inside and just above a canyon of aspect ratio 1.0. The left panel shows the vector field inside the canyon for the mechanically driven flow ( $B = 0$ ) and the right panel shows the vector field inside the canyon when the flow is buoyancy dominated ( $B = 400$ ). The buoyancy flux at the leeward wall causes the vortex to extend above the canyon. The buoyant air near the wall rises and the resulting mixing causes entrainment of air towards the wall. This increases the air speeds within the canyon. To clarify distinctly the effects of the heated wall simulations where  $U_0 = 0$  ( $B$  goes to infinity), the flow field for this case is shown in Fig. 4. The heated left wall leads to natural convection from the wall. In a thin boundary layer ( $\sim 0.05 H$ ) next to the wall a thermally driven plume is formed that rises up above the canyon. Air is entrained into the plume from both sides. The entrainment of air into the plume inside the canyon leads to a formation of a thermally driven vortex as the figure shows. Thus in the case with a heated leeward wall, the mechanical and the buoyancy flow will support each other.

The CFD simulations are validated against field data (Dallman et al. [7]), wind tunnel data (Allegrini et al. [1]) and large eddy simulation (Park et al. [17]) and the results for  $u/U_0$  as a function of  $B$  are displayed in Fig. 5. The aspect ratio of the field experimental canyon is 0.67, the wind tunnel is 1.0 and the LES is also 1.0. The field experiment data encompasses  $B \leq 1$ . When  $B$  is about 0.1, the value of  $u$  starts increasing, indicating that  $B_c$  is about 0.1. The flow is not believed to reach the buoyancy dominant regime for the field data. The wind tunnel data have  $B$  values between 0 and 10. The data show an obvious increase of  $u$  with increased  $B$ . The CFD results show the same trend as the wind tunnel and field data. From the CFD simulations the flow is considered mechanically driven until  $B$  is larger than 0.1 ( $B_c = 0.1$ ), below which the increase of  $u$  is negligible. When  $B$  is larger than about 0.1, it is clear that

**Fig. 4** The special case when  $U_0 = 0$  ( $B$  goes to infinity). The heated left wall creates a thermally driven vortex inside the canyon.  $v_{max}$  is the maximum measured velocity inside the canyon

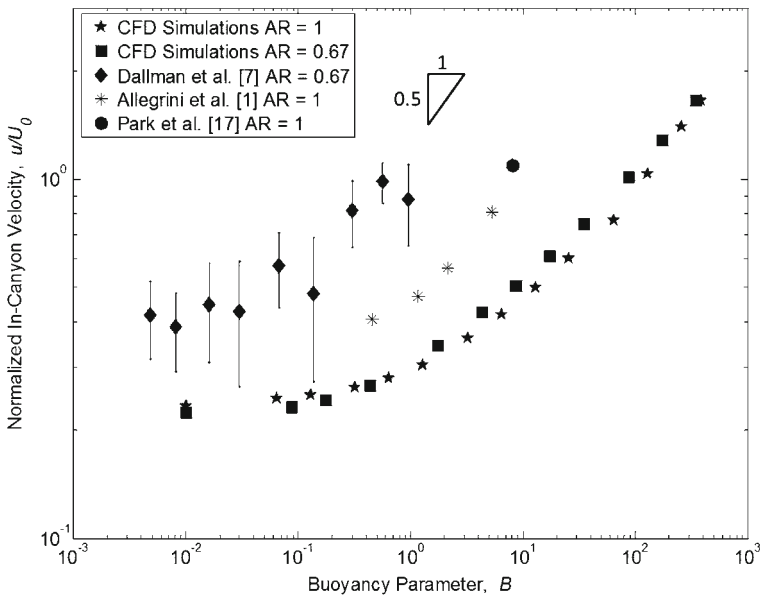
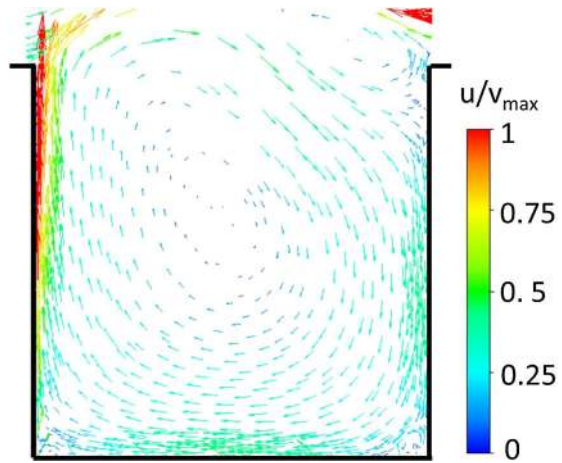


**Fig. 5** Comparison of current CFD simulations with wind tunnel data [1], field data [7] and large eddy simulations results [17]. The fit shows the  $u/U_0 \sim B^{1/2}$  behavior

$u$  increases with  $B$ . To determine the  $B_t$  and  $b_2$  parameters from Eq. 9, the least square fit is used on the data set. It indicates that the flow is in the intermediate regime up to  $B = 50$  ( $B_t = 50$ ) and thus completely buoyancy driven when  $B \geq 50$ . Figure 5 shows how  $u/U_0$  increases by  $B$  raised to the power of about 0.5 as theoretically predicted for canyons with aspect ratios 0.67 and 1. Owing to weather conditions in the real environment and operational difficulties in wind tunnels, it is unlikely that the buoyancy dominant flow regime would be reached. Thus the wind tunnel data and the experimental results show only the mechanically driven and intermediate regimes, and the CFD has the advantage of extending the  $B$  range and crossing into the purely buoyancy driven regime.

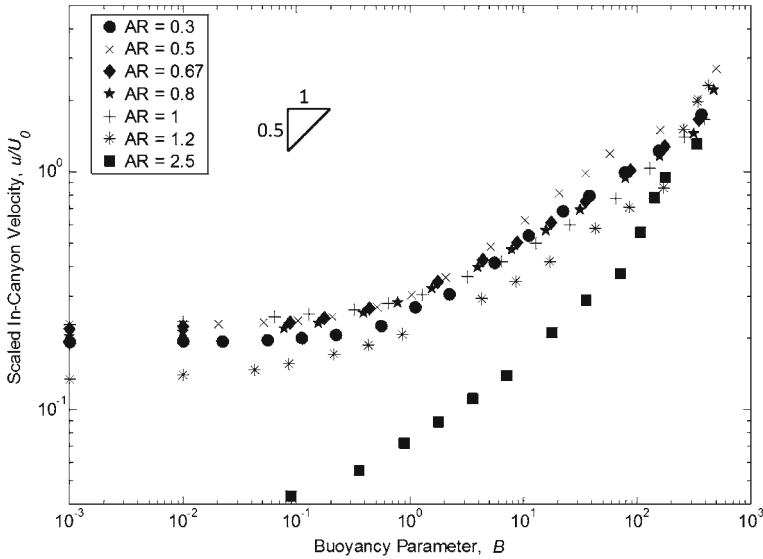


**Fig. 6** Normalized  $u$  as a function of  $B$  for canyons of seven different aspect ratios

The aspect ratio is a critical factor that affects the vortex formation and the relative role of mechanical and thermal forcing. CFD simulations were performed on canyons with seven aspect ratios and the results are shown in Fig. 6. It shows some consistency in the development of  $u/U_0$  with  $B$  for canyons with aspect ratios 0.3–1.2 but for the canyon with an aspect ratio of 2.5,  $u/U_0$  is relatively lower in the mechanical and transitional regimes but increases more rapidly once the buoyancy dominant regime is reached at  $B = 50$ . This may be due to increased frictional resistance to the flow inside the deep canyon. To show how the aspect ratio of the canyons affect the thermal exponent,  $b_2$ , introduced in Eq. (9) and theoretically predicted to be 0.5 in Dallman et al. [7],  $b_2$  is plotted as a function of aspect ratio in Fig. 7. The  $b_2$  parameter is determined by using the least square fit on the data when the flow is considered to be buoyancy driven ( $B$  larger than 50). As seen in the figure, for canyons of aspect ratios between 0.67 and 1.0,  $u/U_0$  increases as a function of the  $B$  parameter raised to the power of roughly 0.5, which is consistent with the theoretical considerations. For canyons of lower aspect ratios,  $u/U_0$  increases with  $B$  raised to the power of about 0.35 and for canyon of aspect ratios larger than 1.0, the exponent on the  $B$  parameter is larger than predicted in the theoretical considerations. The theoretical derivation of the relationship between  $u/U_0$  and the  $B$  parameter was done for canyons in the skimming flow regime with one rotating vortex centered in the middle of the canyon. CFD simulations were also performed on canyons with aspect ratios 0.3 and 2.5. These two canyons are only included in this study to consider extreme cases and show the effects of the different aspect ratios on the air flow. A canyon with an aspect ratio 0.3 is in the isolated roughness flow regime (Oke [16]) with the center of the vortex near the windward wall, while a canyon with an aspect ratio 2.5 has two vortices, stacked upon each other. The lower vortex is formed because of increased frictional resistance to the flow inside the deep canyon. When the leeward wall of the deep canyon is heated the weak lower vortex disappears and only one vortex is formed where the buoyancy flow overcomes the increased friction inside the canyon. The characteristic velocity used in this study accounts for the lower weaker vortex when the flow is purely mechanically driven, but when the buoyancy is taken into the account by heating the leeward

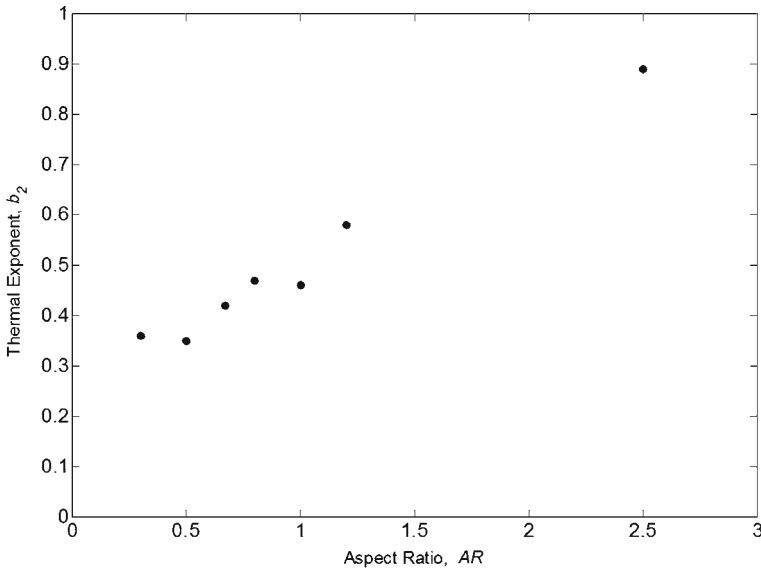


**Fig. 7** The thermal exponent  $b_2$  from Eq. (9) varies with the aspect ratios of the canyons. The theoretical considerations in Dallman et al. [7] seem to hold for the canyons of aspect ratios of 0.8, 1.0 and 1.2

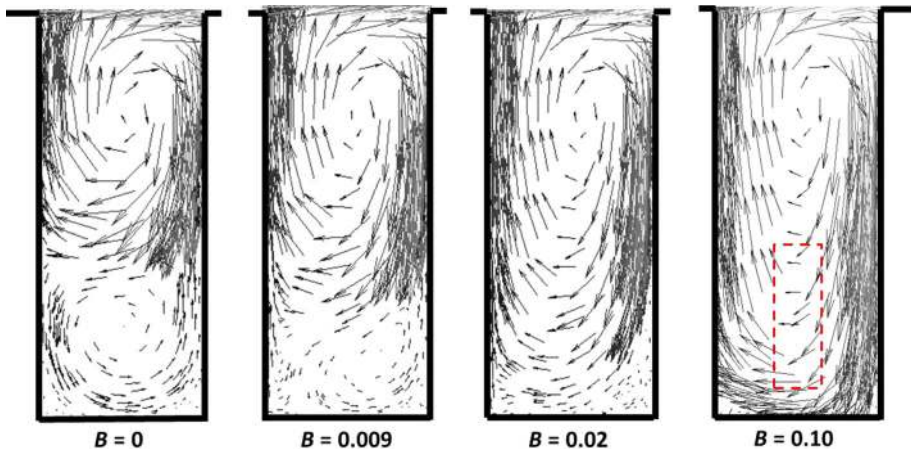


**Fig. 8** The flow structure in the canyons with an aspect ratio 2.5. The lower vortex disappears when  $B$  is equal to 0.02. The red box shows where  $u$  is measured, from 0.1 up to 0.4  $H$  (vertically) and between 0.35 and 0.65  $L$  horizontally)

wall, only one vortex develops and thus  $u$  is consistent and comparable with the canyons with the other aspect ratios. Figure 8 shows how the lower vortex disappears when the  $B$  parameter is increased. The relationship between  $u$  and  $B$  in Dallman et al. [7] is for canyons where only one vortex is formed inside the canyon. For a flow structure in a canyon with an aspect ratio near 1 (Fig. 3), the vortex formed is centered in the middle of the canyon. The thermal effects are greater for canyons with larger aspect ratios, because of larger areas over which buoyancy can influence and increase the flow. Figures 3 and 8 show the domain where averaging of  $u$  is performed as dashed-line boxes.

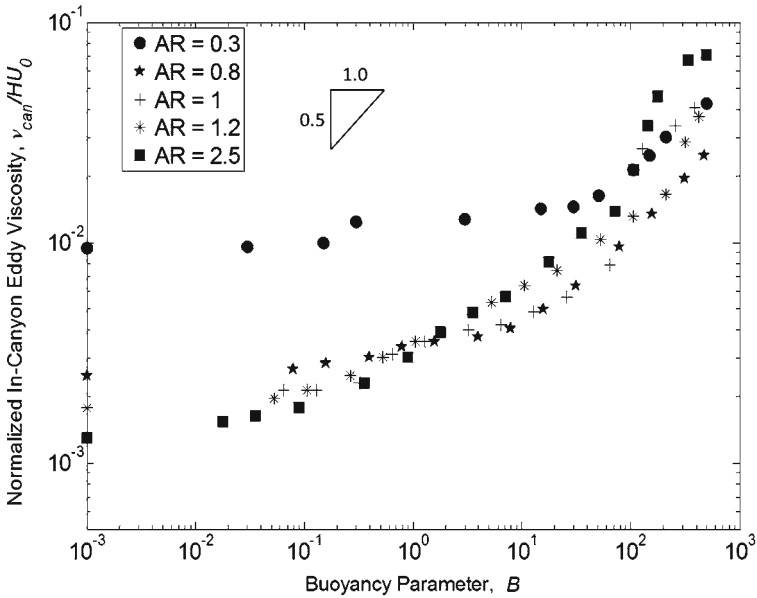


**Fig. 9** Development of normalized in-canyon eddy viscosity with  $B$ . The buoyancy effects are more important in determining  $v_{can}$  in deeper canyons (larger aspect ratios)

Human exposure to air pollutants is an important factor in determining quality of life in urban areas. The magnitude of turbulence (eddy) viscosity inside the canyon,  $v_{can}$ , indicates the amount of mixing between in-canyon air and ambient air above it and thus the efficiency of the pollutant removal from the canyon. The normalized average  $v_{can}$  inside the canyons is shown in Fig. 9. The results show that  $v_{can}/U_0H$  increases with increasing  $B$  parameter. The buoyancy effects on the turbulence viscosity also increase with increased aspect ratio. The increase in  $v_{can}/U_0H$  between the mechanical case and the largest  $B$  value is tenfold. This shows the importance of including thermal situations when simulating air quality in urban areas.

### 6 Conclusions

Mechanically driven vortices can be developed in urban canyons when there is strong advection of ambient air above the city. In addition, solar and thermal radiation can heat the buildings’ exterior walls far above the ambient air temperature. The heat flux near the walls can generate significant amounts of buoyancy. In this study a purely thermally driven flow inside a street canyon was examined and the influence of the leeward wall heating on the mechanically driven vortex inside urban canyons by performing CFD simulations over a wide parameter range were considered. The differential wall heating leads to a buoyancy-driven flow that affects the flow field inside the urban street canyon. A dimensionless buoyancy parameter  $B$  is used to characterize the changes in the flow regime under different amounts of wall heating. The  $B$  parameter also incorporates the effects of canyon geometry and advection strength above the city, for a particular type of (single-cell) flow structure. Steady-state simulations with a CFD code show that buoyancy can have significant effects on vortices formed inside urban canyons. The magnitude of this effect is dependent on the  $B$  parameter,

which was varied between 0 and about 500 in this study. The CFD simulations were compared with theoretical considerations. The best match is for canyons of aspect ratios 0.67–1.0. The simulations show that the geometry of the canyon affects the in-canyon velocity magnitude as  $B$  varies. This occurs despite the fact that  $B$  includes the aspect ratio of the canyon. The simulations indicate that the flow is purely buoyancy driven when the  $B$  parameter of the flow is larger than 50.

A typical urban area geometry can consist of 3–4 floor story buildings, reaching at least 10 m height and an aspect ratio of about unity. For mild synoptic wind speeds of about  $1.0 \text{ ms}^{-1}$  and the wall temperature difference of about 10 K,  $B$  is on the order of 1.0–10. Lower synoptic wind speeds increase the magnitude of  $B$  and enhance the relative importance of buoyancy. For the geometry and temperature difference considered, the urban air flow is purely mechanically driven when  $U_0$  is larger than  $4.0 \text{ ms}^{-1}$ , purely buoyancy driven when the flow is less than  $0.2 \text{ ms}^{-1}$  and thus in the intermediate regime there between. In warm regimes, such as Southeast Asia and the Middle East the buoyancy force inside the urban environment can clearly play a critical role in determining the air flow and dispersion of pollutants out of the urban environment and thus on human exposure to air pollutants. In a separated paper, the effects of the buoyancy force on the air exchange between the in-canyon and ambient air will be considered. It is an important factor in determining the air quality within the built urban environments and thus in determining the human exposure to air pollutants.

The increase of the normalized eddy viscosity,  $v_{can}/U_0H$ , with increased  $B$  suggests that buoyancy plays a critical role in pollutant removal from urban street canyons during calm and sunny days. The increase in turbulence viscosity is higher in the deep canyons than in the shallow canyons. Thus, when modeling for pollutant removal and distribution, it is necessary to account for the buoyancy force.

Future studies should also consider simulations that model the unsteadiness of ambient free stream wind under conditions where the buoyancy driven flow is dominant. Does the unsteadiness of flow direction and magnitude predominantly overcome the buoyant effects?

**Acknowledgments** This research was supported by the Singapore National Research Foundation through the Singapore-MIT Alliance for Research and Technology's Center for Environmental Sensing and Modeling (CENSAM). During the preparation of this paper, H.J.S. Fernando was supported by National Science Foundation (CMG; Grant # 0934592). The authors would like to thank the two reviewers for their useful comments and suggestions.

## References

1. Allegrini J, Dorer V, Carmeliet J (2013) Wind tunnel measurements of buoyant flows in street canyons. *Build Environ* 59:315–326
2. ANSYS Inc. (2012) ANSYS Fluent 14.0 Theory Guide
3. Britter RE, Hanna SR (2003) Flow and dispersion in urban areas. *Ann Rev Fluid Mech* 35(1):469–496
4. Cai X (2012) Effects of wall heating on flow characteristics in a street canyon. *Bound-Lay Meteorol* 142(3):443–467
5. Cai X (2012) Effects of differential wall heating in street canyons on dispersion and ventilation characteristics of a passive scalar. *Atmos Environ* 51:268–277
6. Castro IP, Robins AG (1977) The flow around a surface-mounted cube in uniform and turbulent streams. *J Fluid Mech* 79(02):307–335
7. Dallman A, Magnusson S, Britter RE, Norford L, Entekhabi D, Fernando HJS (2014) Conditions for thermal circulation in urban street canyons. *Build Environ*
8. Department of Economic and Social Affairs (UN DESA). (2012) World Urbanization Prospects 2011 highlights. Technology. <http://www.slideshare.net/undesa/wup2011-highlights> Accessed 30 Apr 2012

9. Fernando HJS, Zajic D, Di Sabatino S, Dimitrova R, Hedquist B, Dallman A (2010) Flow, turbulence, and pollutant dispersion in urban atmospheres. *Phys Fluids* 22(5):051301
10. Kim JJ, Baik JJ (1999) A numerical study of thermal effects on flow and pollutant dispersion in urban street canyons. *J Appl Meteorol* 38(9):1249–1261
11. Kim JJ, Baik JJ (2004) A numerical study of the effects of ambient wind direction on flow and dispersion in urban street canyons using the RNG  $k-\epsilon$  turbulence model. *Atmos Environ* 38(19):3039–3048
12. Li XX, Britter RE, Koh TY, Norford L, Liu CH, Entekhabi D, Leung DYC (2010) Large-Eddy simulation of flow and pollutant transport in urban street canyons with ground heating. *Bound-Lay Meteorol* 137(2):187–204
13. Li XX, Britter RE, Norford L, Koh TY, Entekhabi D (2012) Flow and pollutant transport in urban street canyons of different aspect ratios with ground heating: Large-Eddy simulation. *Bound-Lay Meteorol* 142:289–304
14. Look P, Belcher S, Harrison R (2000) Coupling between air flow in streets and the well-developed boundary layer aloft. *Atmos Environ* 34(16):2613–2621
15. Louka P, Vachon G, Sini JF, Mestayer PG, Rosant JM (2002) Thermal effects on the airflow in a street canyon—Nantes’99 experimental results and model simulations. *Water Air Soil Pollut* 2(5–6):351–364
16. Oke TR (1988) Street design and urban canopy layer climate. *Energy Build* 11(1):103
17. Park SB, Baik JJ, Raasch S, Letzel MO (2012) A Large-Eddy simulation study of thermal effects on turbulent flow and dispersion in and above a street canyon. *J Appl Meteorol Climatol* 51(5):829–841
18. Richards PJ, Hoxey RP (1993) Appropriate boundary conditions for computational wind engineering models using the  $k - \epsilon$  turbulence model. *J Wind Eng Ind Aerodyn* 46–47:145–153
19. Sini JF, Anquetin S, Mestayer PG (1996) Pollutant dispersion and thermal effects in urban street canyons. *Atmos Environ* 30(15):2659–2677
20. Solazzo E, Britter RE (2007) Transfer processes in a simulated urban street canyon. *Bound-Lay Meteorol* 124(1):43
21. Stull RB (1988) *An Introduction to boundary layer meteorology*. Springer, Berlin and New York
22. Turner JS (1979) *Buoyancy effects in fluids*. Cambridge University Press, Cambridge